Astron. Astrophys. 363, 1106–1114 (2000)

ASTRONOMY AND ASTROPHYSICS

Resonance line scattering polarization in optically thin planar equatorial disks

R. Ignace

Department of Physics and Astronomy, 203 Van Allen Hall, University of Iowa, Iowa City, IA 52242, USA

Received 21 August 2000 / Accepted 9 October 2000

Abstract. This paper is the third in a series on the anisotropic scattering by optically thin resonance lines in extended stellar envelopes. Considered here is the *polarization* arising from resonance line scattering in equatorial disks. The shape of the polarized line profile is analytically derived under simplifying conditions of constant expansion or rotation for thin lines, with stellar occultation and finite star depolarization effects also included. The polarized profiles for the two cases are radically different. Moreover owing to the symmetries, rotation leads to profiles in both Q_ν and U_ν, whereas only a Q_ν profile survives for an expanding disk, with $U_\nu = 0$ at all Doppler shifts in the line. Retaining the assumption of optical thinness, numerical results are presented for more realistic disk velocity fields: truncated linear expansion and Keplerian rotation. The calculations also include disk absorption of stellar continuum emission. When compared with the simplified analytic cases, many of the gross characteristics of the polarized profiles are retained.

Key words: line: profiles – polarization – stars: early-type – stars: emission-line, Be – stars: rotation

1. Introduction

Circumstellar disks in one form or another appear to be a prevalent and important feature of many stars, such as protostars, Be stars, the evolved B[e] stars, Luminous Blue Variables, Asymptotic Giant Branch stars, cataclysmic variables, and on galactic scales the Active Galactic Nuclei. Understanding these disks in terms of their accretion properties and mass loss is an important area of current research (the subject is far too broad to list the many important studies regarding disks, but see for example reviews by Papaloizou & Lin 1995 and Lin & Papaloizou 1996 that touch on topics relevant to many disk systems). Consequently, new and improved diagnostic methods are of great benefit for interpreting the observations of disk spectra, which can then be used to constrain and guide theoretical models.

This paper is the third in a series to investigate anisotropic resonance line scattering as a probe of the structure of circumstellar media. As discussed more thoroughly in Paper I (Ignace 1998a), the anisotropic and polarizing effects of scattering by resonance lines was considered by Hamilton (1947), who described how resonance scattering may be treated as a mix of isotropic and dipolar scattering, with the parameter $E_1 \in [0, 1]$ characterizing the fraction of the total scattering that is dipolar (see also Chandrasekhar 1960). Hence, $E_1 = 0$ is pure isotropic scattering, whereas $E_1 = 1$ is pure dipole scattering, like that of free electrons.

In Paper I, anisotropic line scattering in spherically expanding winds was discussed, especially of the redshifted emission where absorption can largely be ignored. It was shown that the emission profile shape can be altered by 10% at most for realistic wind models. Of course, there is no net polarization in the line profile for an unresolved spherical source. In Paper II (Ignace 1998b), circumstellar disks were considered. Unlike the spherical case where viewing inclination is arbitrary, it was shown that interesting profile effects can be expected of equatorial disks. However, only the total emission profile was modelled. This third paper extends the work on disks to report on polarized emission profiles [1].

The continuum polarization that arises from electron scattering in equatorial disks has been considered in numerous papers. Especially popular have been studies of Be star disks (Brown & McLean 1977; Brown & Fox 1989; Fox & Brown 1991; Fox 1991; Bjorkman & Bjorkman 1994; Wood et al. 1997 to name a few). Relatively few papers have focussed on the polarization of line profiles in stellar winds, some exceptions being Caroff et al. (1972), McLean (1979), Poeckert & Marlborough (1978), McKenna (1984, 1985), Jeffery (1989, 1990), Wood & Brown (1994ab), Brown & Wood (1994), and Harries (2000). And of these, only a couple were concerned with polarization arising from resonance line scattering (although it is worth noting that quite sophisticated advances in line scattering polarization have been considered in static and plane-parallel geometries, such as Trujillo Bueno & Manso Sainz 1999 and Rangarajan 1999). However, polarized line profiles potentially contain a wealth of important information about the disk structure. The scattering

Send offprint requests to: ri@astro.physics.uiowa.edu

[1] Ignace et al. (1999) have examined a simple case involving optically thin polarized line profiles from planar equatorial disks in constant expansion, but the focus there was on a magnetic diagnostic method called the "Hanle Effect". In their study the star was treated as a point source of illumination, with finite star effects being ignored.

geometry relates directly to (a) the Doppler shifted frequency at which resonance scattered light will appear in the profile and (b) its polarization.

In Sect. 2, emission profile shapes are derived for optically thin planar disks in pure expansion or rotation. Initially the expansion and rotation are assumed constant leading to analytic expressions for the profile shape. Numerical profile calculations are also given for disks in linear expansion or Keplerian rotation. A discussion of the results for observations and directions for further study are presented in Sect. 3.

2. Resonance line scattering polarization in planar equatorial disks

In deriving the emission profiles from equatorial disks, several assumptions are made, as follows:

1. The intrinsic line profile is treated as a delta function in frequency.
2. The line is optically thin.
3. The disk is axisymmetric and planar at the equator, hence a delta function along the symmetry axis, z_* (see Figs. 1 and 2 of Paper II).
4. Only pure radial expansion or rotation are treated.

This restrictive set of assumptions allows to focus on the effects of the E_1 parameter, viewing inclination i, and the disk velocity field for the polarized line profiles.

The notation and formalism of Paper II are adopted. The new considerations revolve around the polarized flux Q_ν and U_ν. By symmetry, the Stokes U_ν flux is zero for an expanding disk since it is left-right symmetric with respect to the viewing sightline. However, for rotation, the disk is back-front symmetric only if the star is approximated as a point source of illumination. Occultation by the finite sized star breaks that symmetry, and so a net U_ν flux is generally to be expected for a rotating disk, which will be shown below.

2.1. General expressions for optically thin polarized line profiles in equatorial disks

Assuming optically thin line emission, the Stokes fluxes F_ν, Q_ν, and U_ν observed at frequency $\nu_{\rm obs}$ in the profile corresponding to velocity shift $v_{\rm z} = v_{\rm obs}$ is given by a volume integral over the isovelocity zone. Consider a star of luminosity L_ν, distance D, and radius R_*. Light emanating from the star is scattered in a disk with surface density Σ. The disk is permitted to have a velocity field of the form $(w_{\rm R}, w_\varphi) = (v_{\rm max}\sin i)^{-1}\,(v_{\rm R}, v_\varphi)$, where $v_{\rm max}$ is some appropriate normalization constant for the speed distributions $v_{\rm R}$ and v_φ, the angle i is the viewing inclination of the disk, and cylindrical coordinates (R, φ) are used. Introducing a normalized cylindrical radius $\varpi = R/R_*$, the Stokes fluxes will then be

$$\frac{F_\nu}{F_0} = \int_{w_{\rm z}} \left[\tilde{J}_\nu - \frac{1}{8}E_1(3\tilde{K}_\nu - \tilde{J}_\nu)(1 - 3\sin^2 i\,\cos^2\varphi_0)\right] \times |w_{\rm R}\,\sin\varphi_0 + w_\varphi\,\cos\varphi_0|^{-1}\,(\Sigma/\Sigma_0)\,\varpi\,d\varpi, \quad (1)$$

$$\frac{Q_\nu}{F_0} = \frac{3}{16}E_1\int_{w_{\rm z}}(3\tilde{K}_\nu - \tilde{J}_\nu) \times \left[\sin^2 i - (1+\cos^2 i)\,\cos(2\varphi_0)\right] \times |w_{\rm R}\,\sin\varphi_0 + w_\varphi\,\cos\varphi_0|^{-1}\,(\Sigma/\Sigma_0)\,\varpi\,d\varpi, \quad (2)$$

and

$$\frac{U_\nu}{F_0} = \frac{3}{8}E_1\int_{w_{\rm z}}(3\tilde{K}_\nu - \tilde{J}_\nu)\,\cos i\,\sin(2\varphi_0) \times |w_{\rm R}\sin\varphi_0 + w_\varphi\cos\varphi_0|^{-1}\,(\Sigma/\Sigma_0)\,\varpi\,d\varpi. \quad (3)$$

The angle $\varphi_0 = \varphi_0(\varpi)$ describes the locus of points in the disk for which $w_{\rm z} = constant$ (see Paper II). The variable Σ_0 is a scaling parameter of the disk surface density so that Σ/Σ_0 is a function of ϖ only. For a resonance line at wavelength $\lambda_{\rm ul}$ with a cross section σ_l, the various constants have been collected into the parameter $F_0 = L_\nu\,\sigma_l\,\Sigma_0\,\lambda_{\rm ul}/8\pi\,D^2\,v_{\rm max}\sin i$. The normalized Eddington moments $\tilde{J}_\nu$ and $\tilde{K}_\nu$ are J_ν and K_ν divided by $L_*/16\pi^2{R_*}^2$. Note that the value of F_0 will vary from line to line.

2.2. Line profiles from disks in constant expansion or rotation

Assuming either constant expansion or rotation, the disk velocity field takes the form of $v_{\rm R} = v_{\rm max}$ and $v_\varphi = 0$, or $v_{\rm R} = 0$ and $v_\varphi = v_{\rm max}$. Thus $w_{\rm R}$ and w_φ are either 0 or 1, and the observed Doppler shift toward the observer depends only on azimuth as

$$w_{\rm z} = w_{\rm R}\,\cos\varphi_0 + w_\varphi\,\sin\varphi_0. \quad (4)$$

In the following, analytic expressions for the polarized emission profiles from the disk are derived for resonance line scattering. The simple case of a point source of illumination is derived first, followed by a consideration of the finite star effects of stellar occultation and finite star depolarization.

2.2.1. The point star approximation

Treating the star as a point source of illumination implies $\tilde{J}_\nu = \tilde{K}_\nu = \varpi^{-2}$. Taking the disk density to be $\Sigma = \Sigma_0\,\varpi^{-1}$ and noting that isovelocity zones correspond to $\varphi_0 = constant$, the Stokes flux relations reduce to the forms

$$\frac{F_\nu}{F_0} = |w_{\rm R}\,\sin\varphi_0 + w_\varphi\,\cos\varphi_0|^{-1} \times \left[1 - \frac{1}{4}E_1\,(1 - 3\sin^2 i\cos^2\varphi_0)\right], \quad (5)$$

$$\frac{Q_\nu}{F_0} = |w_{\rm R}\,\sin\varphi_0 + w_\varphi\,\cos\varphi_0|^{-1} \times \frac{3}{8}E_1\left[\sin^2 i - (1+\cos^2 i)\,\cos 2\varphi_0\right] \quad (6)$$

and

$$U_\nu = 0. \quad (7)$$

Since only pure expansion or pure rotation is considered, the denominator involving the disk velocity field ultimately reduces to $\sqrt{1 - w_{\rm z}^2}$.

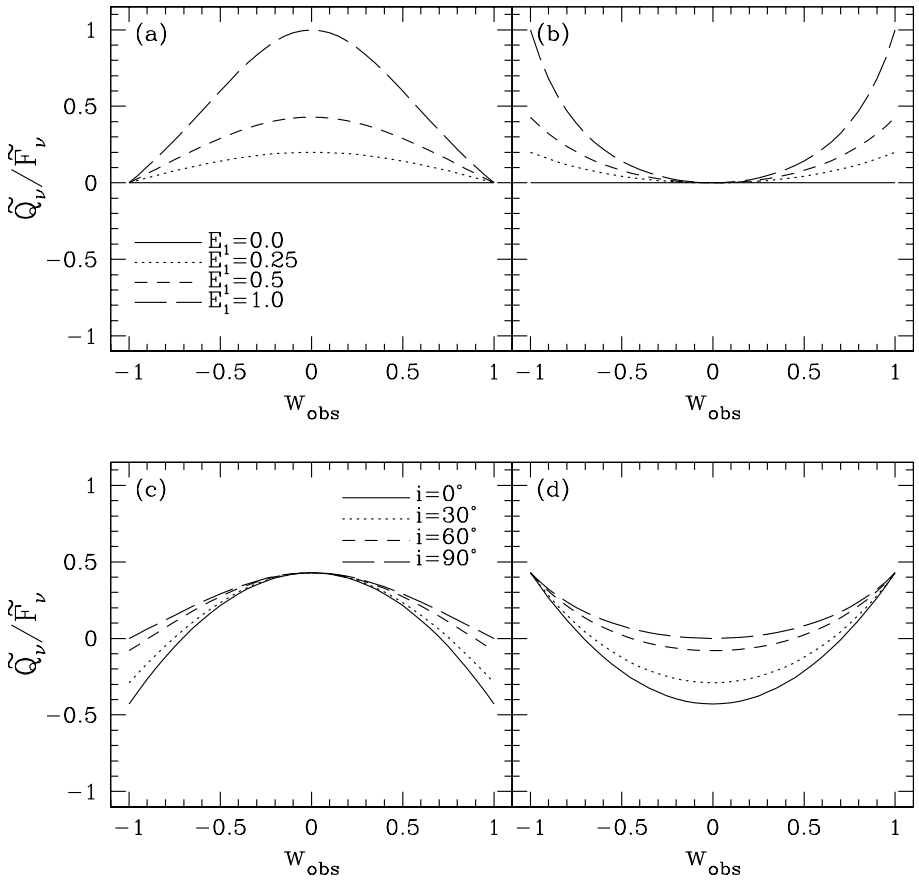

Fig. 1a–d. A comparison of the polarized emission profiles (given as fractional polarizations) for equatorial planar disks in constant expansion (left panels **a** and **c**) versus ones with constant rotation (right panels **b** and **d**). The upper panels are for edge-on viewing perspectives with $i = 90^\circ$ but E_1 allowed to vary as indicated. Lower panels are for $E_1 = 0.5$ but different viewing inclinations. The primary morphological difference between the two cases is that expansion yields concave down profiles whereas rotation yields concave up profiles.

The total polarized line profile is defined to be

$$p_l = \frac{\sqrt{Q_\nu^2 + U_\nu^2}}{F_\nu}, \tag{8}$$

which for $U_\nu = 0$ reduces to

$$p_l = \frac{3}{8} E_1 \frac{\sin^2 i - (1 + \cos^2 i)\, \cos 2\varphi}{1 - \frac{1}{4} E_1 \,(1 - 3 \sin^2 i \, \cos^2 \varphi)}. \tag{9}$$

The "0" subscript on φ has been dropped. Clearly the numerator can be positive or negative. Polarization is normally positive definite, but here the sign is used to indicate the position angle orientation of the polarization, with positive $(+)$ signifying a polarization parallel to the disk symmetry axis and negative $(-)$ indicating one that is orthogonal to that axis. Note that the polarization in Eq. (9) is normalized by the emission line flux only – the continuum or "direct" contribution to the flux by the star has not been included. Fig. 1 shows plots of polarized line profiles from Eq. (9) as fractional polarizations for various values of E_1 and viewing inclinations i. Expanding disks in (a) and (c) give polarized profiles that are concave down in shape, but rotating disks (b) and (d) are concave up.

In the case of low spectral resolution data, it is useful to consider the line integrated polarization

$$p_{\rm tot} = \frac{\int \tilde{Q}_\nu \, dw_{\rm z}}{\int \tilde{F}_\nu \, dw_{\rm z}} = \frac{3\, E_1 \, \sin^2 i}{2(4 - E_1) + 3\, E_1 \, \sin^2 i}, \tag{10}$$

which is a function of E_1 and inclination i only. Fig. 2 shows the run of $p_{\rm tot}$ plotted against E_1. The curves are for different values of $\sin^2 i$ ranging from 0 to 1 in steps of 0.2. Generally, one will know from atomic physics the E_1 value for a given line transition, so that a plot like Fig. 2 could then be used to determine the disk viewing inclination from a measurement of the total line polarization. A similar consideration can be used by measuring the continuum electron scattering polarization; however, the electron scattering optical depth must be known (see Brown & McLean 1977). The advantage of the resonance line is that the line optical depth (if optically thin) will cancel out when taking the ratio of polarized line flux to total line flux (i.e., not including the continuum emission). A disadvantage is that it can be difficult to set the continuum level, and so the line flux measurement may have substantial error. Moreover, the effects of absorption, stellar occultation, and finite star depolarization have so far been neglected.

2.2.2. Finite star effects

If the scattering region extends down to the stellar radius, then occultation cannot be ignored. The lower boundary to the integration over cylindrical radius in Eqs. (1)–(3) is now a function of the Doppler shift in the profile and the viewing inclination. The problem is to determine where rays intersect the disk if tangent to the stellar photosphere and to relate that locus of points to the corresponding line-of-sight Doppler shift. The geometri-

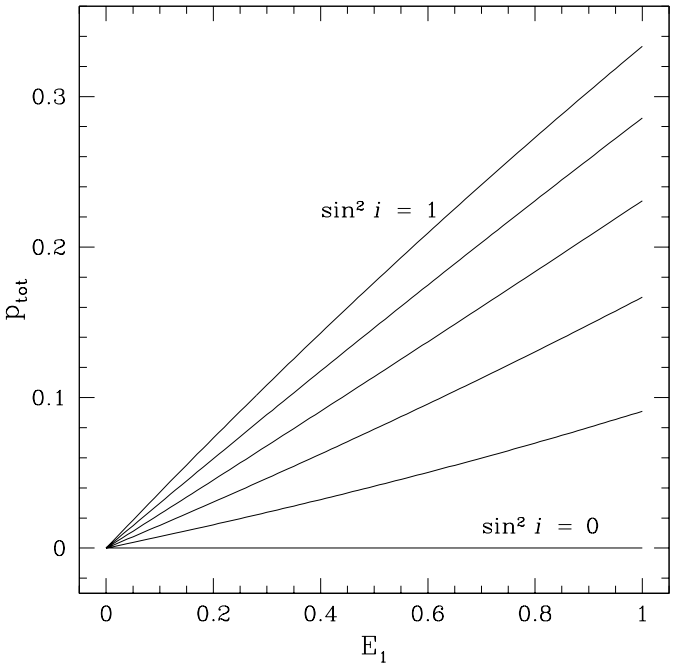

Fig. 2. Shown is the line integrated polarization $p_{\rm tot}$ plotted as a function of E_1, with each different curve corresponding to a value of $\sin^2 i = 0, 0.2, 0.4, 0.6, 0.8$, and 1.0. These curves are for the simplified case of a point source star and a disk in either constant expansion or rotation, yet the figure illustrates how resonance scattering polarization with even low spectral resolution data might be used to infer the disk viewing inclination. As long as the line is optically thin, these curves are independent of the line optical depth (see the text).

cal solution has been discussed by Fox & Brown (1991) who derived

$$\varpi_0 = \left(1 - \sin^2 i \cos^2 \varphi\right)^{-1/2}, \tag{11}$$

which traces the projection of the stellar limb onto the disk. It is straightforward to relate ϖ_0 to $w_{\rm z}$ using Eq. (4) for the dependence of Doppler shift on azimuth $\varphi = \varphi_0$. For constant expansion, one has $\varpi_0 = (1 - w_{\rm z}^2 \sin^2 i)^{-1/2}$; for pure rotation the solution is $\varpi_0 = (\cos^2 i + w_{\rm z}^2 \sin^2 i)^{-1/2}$.

Another finite star effect, Cassinelli et al. (1987) discussed how the continuum polarization arising from electron scattering can be reduced at small radii where the star cannot be treated as a point source. The reduction of polarization owes to the more nearly isotropic distribution of incident starlight at the scatterer. This same effect holds for the case of resonance line scattering, since the anisotropic scattering is like that of free electrons. Following Cassinelli et al., the depolarization effect is contained within $\tilde{J}_\nu$ and $\tilde{K}_\nu$. Consider for example a uniformly bright stellar disk, the Eddington factors take on the familiar forms of $\tilde{J}_\nu = 2(1 - \cos\theta_*)$ and $\tilde{K}_\nu = \frac{2}{3}(1 - \cos^3\vartheta_*)$, where $\cos\theta_* = \sqrt{1 - \varpi^{-2}}$. If $\varpi = 1$, then $\cos\theta_* = 0$ and $3\tilde{K}_\nu - \tilde{J}_\nu = 0$ making the polarization contribution in Eqs. (2)–(3) vanish.

Even with occultation and finite star depolarization, the expressions for the Stokes parameters for the emission profile shape can be derived analytically in the case of constant expansion or rotation. For an expanding disk, occultation affects only the redshifted profile for disk material receding from the observer on the far side of the disk. The blueshifted emission does not suffer from occultation, and the expressions for the flux and polarization (noting that $\tilde{U}_\nu = 0$ by symmetry) are

$$\tilde{F}_\nu^{\rm exp} = \left(\frac{\pi - 2}{2}\right)\left[1 - \frac{\pi/16}{\pi - 2} E_1 \left(1 - 3 w_{\rm z}^2 \sin^2 i\right)\right], \tag{12}$$

$$\tilde{Q}_\nu^{\rm exp} = \frac{3\pi}{32} E_1 \left[1 - w_{\rm z}^2 \left(1 + \cos^2 i\right)\right]. \tag{13}$$

For the redshifted side of the profile, the flux and polarization are given by

$$\tilde{F}_\nu^{\rm exp} = \left(\sqrt{\varpi_0^2 - 1} - \varpi_0 + \sin^{-1}\varpi_0^{-1}\right) - \frac{1}{16} E_1 \left(1 - 3 w_{\rm z}^2 \sin^2 i\right) \times \left(\varpi_0^{-1}\sqrt{1 - \varpi_0^{-2}} + \sin^{-1}\varpi_0^{-1}\right), \tag{14}$$

$$\tilde{Q}_\nu^{\rm exp} = \frac{3}{16} E_1 \left[1 - w_{\rm z}^2 \left(1 + \cos^2 i\right)\right] \times \left(\varpi_0^{-1}\sqrt{1 - \varpi_0^{-2}} + \sin^{-1}\varpi_0^{-1}\right). \tag{15}$$

Note that if $\varpi_0 = 1$, corresponding to $w_{\rm z} = 0$ or $i = 0$, the expressions for the red wing reduce to the same form as that for the blue wing, as required.

In the case of rotation, one must bear in mind that the isovelocity zones are left-right symmetric about the line-of-sight to the star. Occultation blocks emission from the far side of the disk, so this means that the redshifted and blueshifted profiles are affected equally. Moreover, there now exists a net Stokes U_ν flux. In normalized form, the Stokes fluxes are given by

$$\tilde{F}_\nu^{\rm rot} = \left(\frac{\pi - 2}{4}\right)\left\{1 + \frac{\pi/16}{\pi - 2} E_1 \times \left(1 - 3\cos^2 i - 3 w_{\rm z}^2 \sin^2 i\right) + \frac{2}{\pi - 2}\left(\sqrt{\varpi_0^2 - 1} - \varpi_0 + \sin^{-1}\varpi_0^{-1}\right) + \frac{1/8}{\pi - 2} E_1 \left(1 - 3\cos^2 i - 3 w_{\rm z}^2 \sin^2 i\right) \times \left(\varpi_0^{-1}\sqrt{1 - \varpi_0^{-2}} + \sin^{-1}\varpi_0^{-1}\right)\right\}, \tag{16}$$

$$\tilde{Q}_\nu^{\rm rot} = -\frac{3}{32} E_1 \left[\cos^2 i - w_{\rm z}^2 \left(1 + \cos^2 i\right)\right] \times \left(\frac{\pi}{2} + \varpi_0^{-1}\sqrt{1 - \varpi_0^{-2}} + \sin^{-1}\varpi_0^{-1}\right), \tag{17}$$

$$\tilde{U}_\nu^{\rm rot} = \frac{3}{8} E_1 \, w_{\rm z} \sqrt{1 - w_{\rm z}^2} \cos i \times \left(\frac{\pi}{2} - \sin^{-1}\varpi_0^{-1} - \varpi_0^{-1}\sqrt{1 - \varpi_0^{-2}}\right). \tag{18}$$

Polarized line profiles based on expressions (12)–(18) are shown in Figs. 3 and 4, the latter being for Stokes $\tilde{U}_\nu$ is only

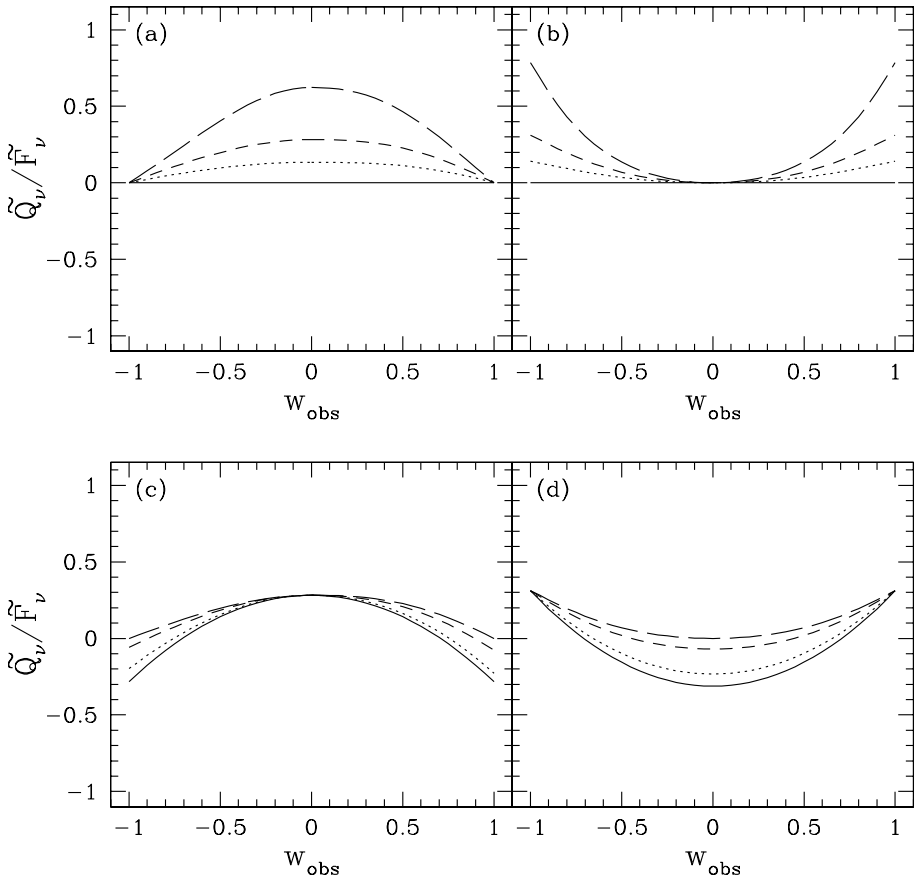

Fig. 3a–d. As in Fig. 1, but now with both stellar occultation and finite star depolarization effects included. The overall effect is to reduce the peak polarizations that are obtained relative to the point star case, and also the polarized profiles for an expanding disk are asymmetric about line center. Note that only for expansion does $p_l = \tilde{Q}_\nu/\tilde{F}_\nu$, whereas a rotating disk also has a Stokes $\tilde{U}_\nu/\tilde{F}_\nu$ profile owing to the effect of stellar occultation (see Fig. 4).

relevant to rotating disks. The format is the same as in Fig. 1. Note that the polarized profiles for the expanding disk case are asymmetric about line center, whereas those for a rotating disk are symmetric. Also in Fig. 4, the $\tilde{U}_\nu$ profiles are antisymmetric, hence the integrated $\tilde{U}_\nu$ flux across the entire line is zero.

2.3. Line profiles from disks in linear expansion or Keplerian rotation

Having derived analytic results for simplified cases to highlight the consequences of anisotropic scattering in disks and the various finite star effects, line profiles for more realistic disk velocity fields are computed in this section. Several assumptions remain, such as axisymmetry and the lines being optically thin, but now absorption of starlight by the intervening disk is also included. Only two specific velocity fields are considered: linear expansion that is truncated at a finite radius and Keplerian rotation.

2.3.1. The case of linear expansion

Line profiles have been computed for a disk that expands linearly as

$$v_{\rm R} = v_\infty \frac{\varpi}{\varpi_{\rm max}} \rightarrow w_{\rm R} = \frac{\varpi}{\varpi_{\rm max}}, \tag{19}$$

where $\varpi_{\rm max}$ represents a transition from linear expansion to constant expansion. Using this velocity parametrization, the isovelocity zones reduce to lines of constant $z = (x_* \sin i)$ in the region of acceleration (see Fig. 1 of Paper I for a sketch detailing the x, z and x_*, z_* coordinates). The surface number density of the disk becomes

$$\Sigma(\varpi) = \Sigma_0 \frac{\varpi_{\rm max}}{\varpi^2}. \tag{20}$$

Fig. 5 shows line profiles for linear expansion using a value of $\varpi_{\rm max} = 10$, beyond which the contribution to the emission by the constant expansion flow is ignored. Results are given for $E_1 = 1$ and three different viewing inclinations of 30°, 60°, and 89° from top to bottom. The latter is chosen because a planar disk viewed perfectly edge-on degenerates to a line as projected against the plane of the sky, an artifact of the disk having no vertical extent. Recall that F_ν is the flux of line emission only, hence the vertical axis is $(F_{\rm c} + F_\nu)/F_{\rm c} = 1 + F_\nu/F_{\rm c}$, for $F_{\rm c}$ the stellar continuum flux outside the line frequencies. At right is the Stokes Q_ν profile now shown as $Q_\nu/(F_{\rm c} + F_\nu)$. (In previous figures, the polarization was given relative to the line emission only, whereas here it is shown relative to the total emission.) Again note that since $U_\nu = 0$, the Stokes Q_ν flux represents the total polarized flux of the line emission.

The total flux emission profiles have already been discussed in Paper II. Basically the blueshifted absorption does little to affect the emission profile; however, stellar occultation of the far side of the disk substantially changes the redshifted profile shape, as is evident from its asymmetry about line center. In contrast, the polarized profile is mostly symmetric, although not

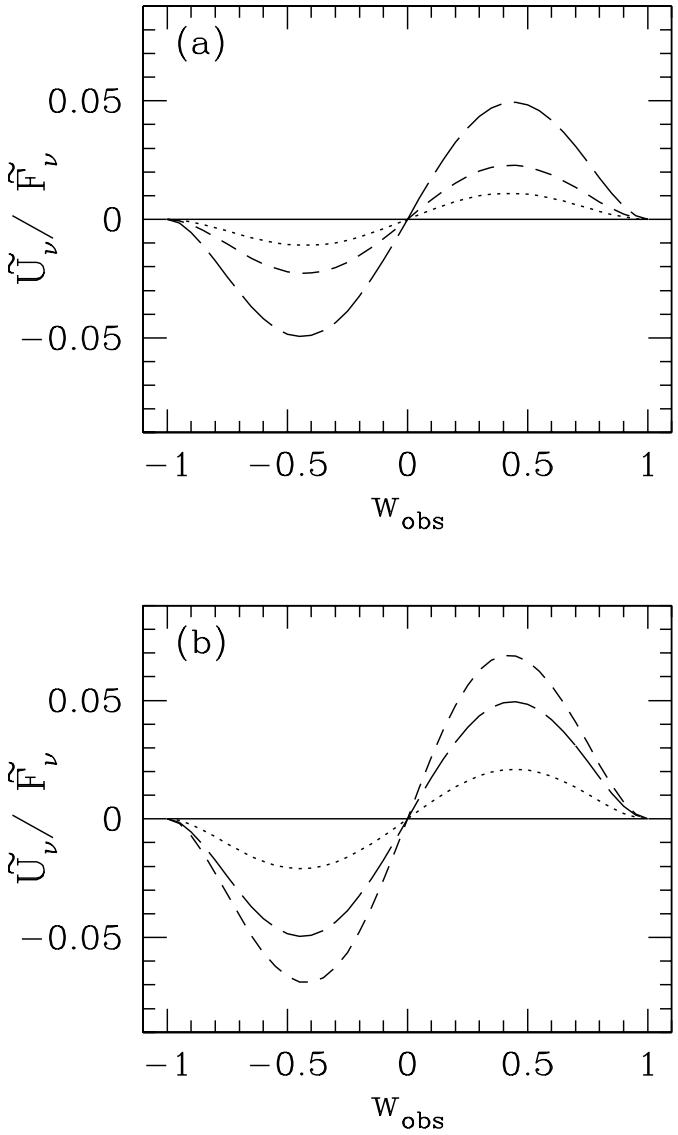

Fig. 4a and b. The $\tilde{U}_\nu/\tilde{F}_\nu$ profile corresponding to the rotating disk case of Fig. 3. Stellar occultation breaks the back-front symmetry associated with a rotating disk, hence a Stokes U_ν flux remains. However, note that the $\tilde{U}_\nu$ profile is antisymmetric about line center so that the line integrated $\tilde{U}_\nu$ flux vanishes.

exactly. It generally maintains the concave down appearance, at least in its central portion, as in the analytic cases of the previous section. Note that all the profiles show similar widths in the plots, but recall that $v_{\rm obs} \propto w_{\rm obs} \sin i$, hence in velocity, frequency, or wavelength units, the emission and polarized profiles in Fig. 5 would appear progressively broader from top to bottom (i.e., for constant $v_{\rm max}$).

2.3.2. The case of Keplerian rotation

The velocity field used for a rotating disk is the Keplerian prescription with

$$v_\varphi = v_{\rm rot}\, \varpi^{-1/2} \rightarrow w_\varphi = \varpi^{-1/2}, \tag{21}$$

where $v_{\rm rot}$ is the equatorial rotation speed. In the case of linear expansion, the isovelocity zones reduce to lines of constant z, but for rotation the topology of the zones is more complicated, with a kind of nested loop pattern. A plot of isovelocity zones is shown in Fig. 2 of Wood & Brown (1994a).

As in Paper II, the disk density is assumed to be of the form

$$\Sigma = \Sigma_0\, \varpi^{-q}, \tag{22}$$

with q positive. So as to make comparison with the expansion case more direct, line profiles have been computed using $q = 2$. For Be star disks, q-values in the range of 2–3 are found from analyses of the disk IR emission (e.g., Waters 1986) and Hα line profile fitting (e.g., Hummel 2000).

Line profiles from a Keplerian disk are shown in Figs. 6 and 7, in the same format as Fig. 5 for the expanding disk case. The profiles from a rotating disk look radically different from those of an expanding disk: both the total emission profiles and the polarized profiles are generally double-peaked. Notice that the central part of the Stokes Q_ν profiles are concave down. Finally, the profiles are symmetric about line center.

The U_ν profiles are displayed in Fig. 7. As in the simplified analytic case, the profiles are antisymmetric about line center, thus yielding no net U_ν flux as integrated across the entire line profile. Also, for nearly edge-on viewing perspectives, U_ν approaches zero at each point in the profile.

3. Discussion

This paper extends results presented in Paper II on anisotropic resonance line scattering profiles to show the polarized emission from such scattering. The main results are that (a) as in Paper II, expanding disks yield line profiles that are asymmetric about line center, whereas those from rotating disks are symmetric, (b) the integrated polarized flux across a resonance line profile will generally be non-zero, so that interesting information about the disk can be derived even from low resolution (i.e., narrow band pass) spectropolarimetry, (c) both Q_ν and U_ν Stokes profiles will be observed in rotating disks, whereas for expanding disks, the U_ν Stokes component will be zero (under the assumptions of axisymmetry) for a suitable orientation of the observer's $Q-U$ measurement axes.

Although these results are quite instructive and may have application to certain restricted cases, numerical simulations for more realistic situations are needed. Of key importance is dropping the assumption of optically thin profiles. To do so will require more sophisticated radiative transfer techniques, as for example the Sobolev method for polarized radiation transport by Jeffery (1990) or techniques based on Monte Carlo simulations.

Since resonance line scattering in its phase scattering properties is so similar to that of Thomson scattering, already one might "guess" at some of the expected effects from scattering in optically thick disks. One naturally expects that at sufficiently large optical depths, multiple scattering will tend to destroy the line polarization. However, Wood et al. (1996) have shown that for Thomson scattering in equatorial disks, the continuum polarization actually increases when the disk moves from opti-

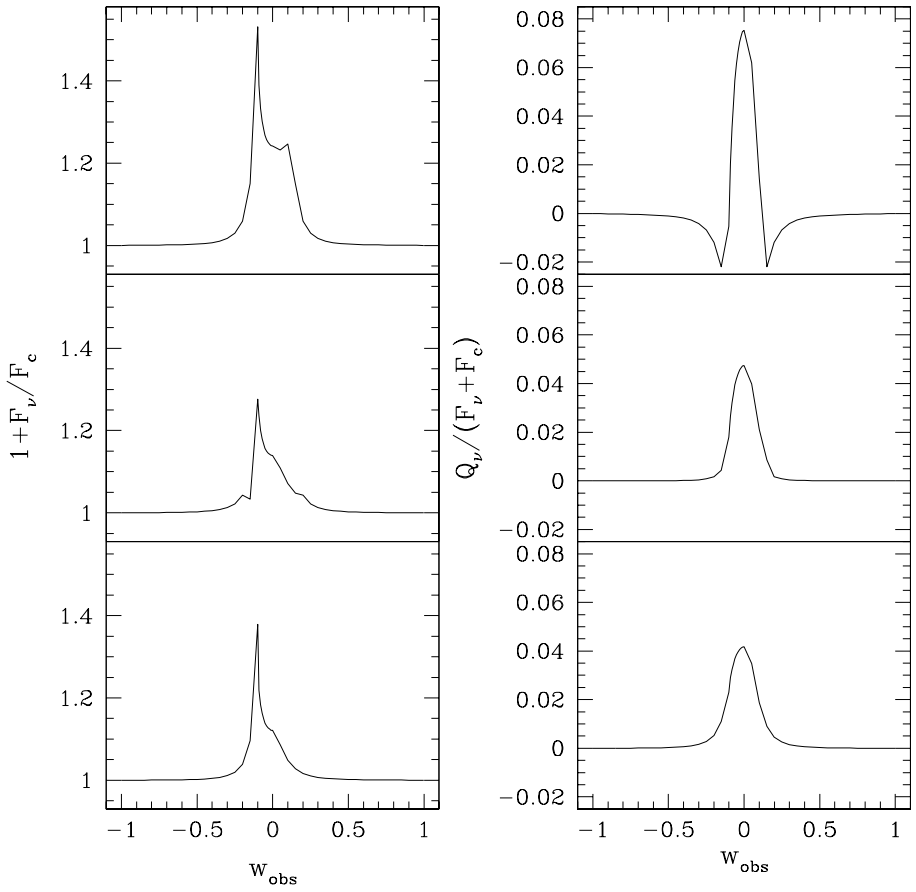

Fig. 5. Emission profiles (left) and polarized profiles (right) from a circumstellar disk undergoing linear expansion. From top to bottom, the viewing inclinations of the disk are $i = 30°$, $60°$, and $89°$. The profiles are asymmetric, especially the blueshifted peak is more prominent than that for the redshifted wing. The polarized profile is concave down at the line core. Note that in distinction to the preceding figures for the analytic examples, the polarized profiles here are shown as Q_ν divided by the total observed flux F_ν for the line and F_c for the direct continuum starlight ($U_\nu = 0$ for expanding disks).

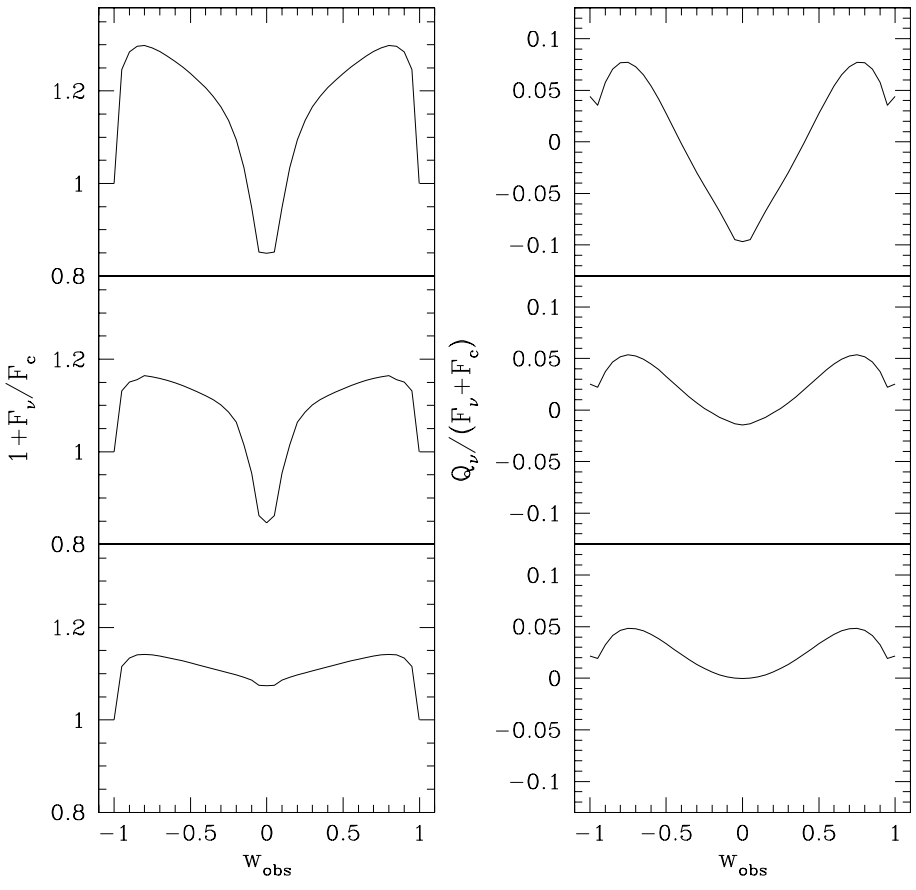

Fig. 6. Similar to Fig. 5, but now for a disk in Keplerian rotation with no radial motion. The profiles are symmetric, and the polarized profiles are concave up at the central region. Note that for rotating disks, stellar occultation leads to a net U_ν polarization, which is shown in Fig. 7.

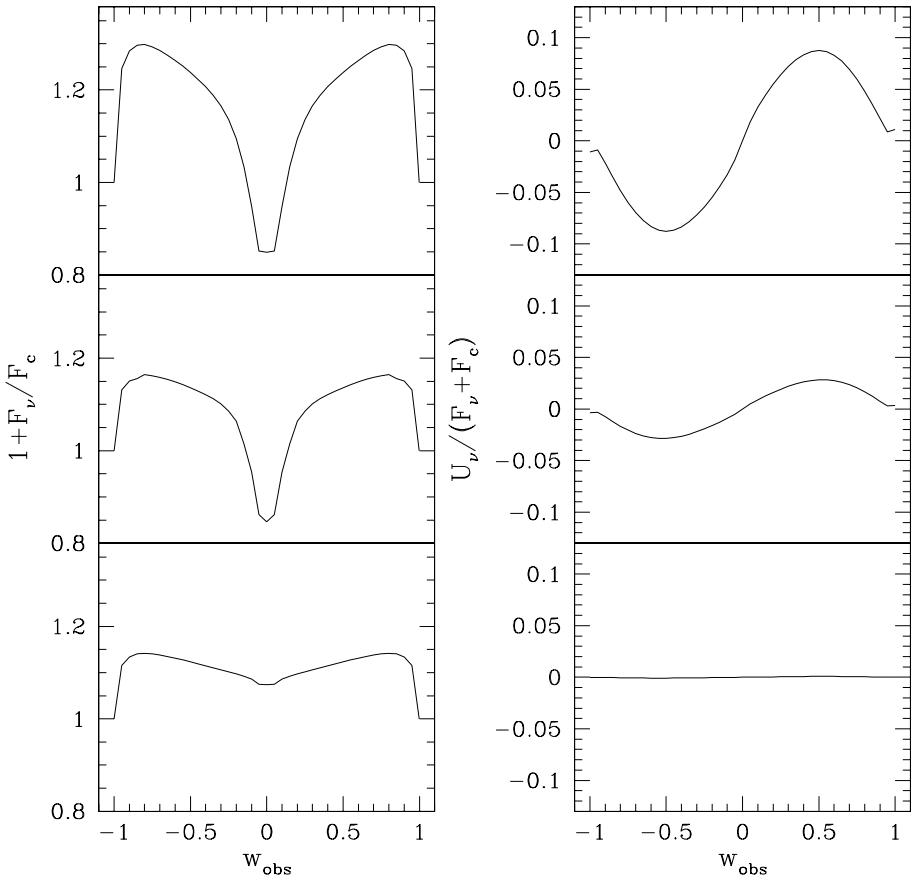

Fig. 7. The U_ν polarization from a disk executing Keplerian rotation. The U_ν flux is antisymmetric about line center. For a nearly edge-on disk, $U_\nu \approx 0$ at each point in the profile, owing to the symmetry of the viewing orientation.

cally thin to optically thick, and then decreases at larger optical depths. A similar effect should likewise be observed for the polarization from resonance line scattering.

An advantage of resonance lines over Thomson scattering is that the polarized emission is spread out across the line profile according to the isovelocity topology, which affords a better opportunity of probing the disk geometry and velocity field. One difficulty in relation to "hot" disks where a substantial fraction of the gas is ionized is that Wood & Bjorkman (1995) have shown that electron scattering will greatly "smear out" the polarized line emission. They were not specifically modelling the effect for resonance line scattering but rather a continuum absorption line. Nonetheless, scattering of polarized resonance line radiation by hot thermal electrons can severely affect the profiles. But note that Thomson scattering has a quite low cross-section of $\sigma_{\rm T} \approx 10^{-24}\,{\rm cm}^{-2}$, whereas resonance lines have cross-sections that can be larger by several orders of magnitude. Hence in disks of relatively low density, the effects of electron scattering may be entirely negligible, yet the polarized emission in suitably chosen lines should be within the realm of current detection thresholds. For example, dedicated monitoring of the polarizations in several Be stars at the Pine Bluff Observatory (Univ. Wisconsin) is easily capable of detecting variations at the 0.1% level (Bjorkman et al. 1997). In general, since resonance line scattering is similar to Thomson scattering in its angular distribution, a given aspherical envelope will yield a similar overall polarization level from line scattering as for electron scattering, the main difference being the scale of the line optical depth as compared to that of the free electrons.

Even if thermal smearing by electron scattering can be ignored, there is the issue of separating the line polarization from that of the continuum. Fortunately, many strong doublets of Li-like atoms that are commonly observed in winds (e.g., CIV 1550) have one component (shorter wavelength) with $E_1 = 0.5$, but the other (longer wavelength) with $E_1 = 0$, the latter producing no polarization from resonance scattering. Thus the Q and U values at the longer wavelength line can be used to disentangle the continuum polarization from that of the line scattering that does contribute at the shorter wavelength component. Indeed in this way, one can correct not only for the electron scattering polarization by the envelope, but also for the ISM contribution. Optical depth effects and the influence of electron scattering are the kinds of issues that must be addressed quantitatively in future studies if resonance line scattering polarization is to be of practical diagnostic value in observations of circumstellar disks.

Acknowledgements. I wish to thank the referee Ruslan Yudin for a careful reading of the text and for comments leading to helpful clarifications.

References

Bjorkman J.E., Bjorkman K.S., 1994, ApJ 436, 818
Bjorkman K.S., Meade M.R., Babler B.L., 1997, BAAS 29, 1275
Brown J.C., McLean S., 1977, A&A 57, 141

Brown J.C., Fox G.K., 1989, ApJ 347, 468
Brown J.C., Wood K., 1994, A&A 290, 634
Caroff L.J., Noerdlinger P.D., Scargle J.D., 1972, ApJ 176, 439
Cassinelli J.P., Nordsieck K.H., Murison M.A., 1987, ApJ 290, 302
Chandrasekhar S., 1960, Radiative Transfer. Dover, New York
Fox G.K., 1991, ApJ 379, 663
Fox G.K., Brown, J.C., 1991, ApJ 375, 300
Hamilton D.R., 1947, ApJ 106, 457
Harries T.J., 2000, MNRAS 315, 722
Hummel W. 2000, to appear in: Smith M.A., Henrichs H.F., Fabregat J. (eds.) The Be Phenomenon in Early-Type Stars. ASP Conf. Series
Ignace R., 1998a, A&A 332, 686
Ignace R., 1998b, A&A 337, 819
Ignace R., Cassinelli J.P., Nordsieck K.H., 1999, ApJ 520, 335
Jeffery D.J., 1989, ApJS 71, 951
Jeffery D.J., 1990, ApJ 352, 267
Lin D.N.C., Papaloizou J.C.B., 1996, ARA&A 34, 703
McKenna S.J., 1984, Ap&SS 106, 283
McKenna S.J., 1985, Ap&SS 108, 31
McLean I.S., 1979, MNRAS 186, 265
Papaloizou J.C.B., Lin D.N.C., 1995, ARA&A 33, 505
Poeckert R., Marlborough J.M., 1978, ApJ 220, 940
Rangarajan K.E., 1999, MNRAS 308, 1053
Trujillo Bueno J., Manso Sainz R., 1999, ApJ 516, 436
Waters L.B.F.M., 1986, A&A 162, 121
Wood K., Brown J.C., 1994a, A&A 285, 220
Wood K., Brown J.C., 1994b, A&A 291, 202
Wood K., Bjorkman J.E., 1995, ApJ 443, 348
Wood K., Bjorkman J.E., Whitney B.A., Code A.D., 1996, ApJ 461, 828
Wood K., Bjorkman K.S., Bjorkman J.E., 1997, ApJ 477, 926